Integration of high resolution geophysical methods. Detection of shallow depth bodies of archaeological interest

Fabio Cammarano([1]), **Paolo Mauriello**([2]), **Domenico Patella**([1])([2]), **Salvatore Piro**([1]), **Francesco Rosso**([1]) **and Lucio Versino**([1])

([1]) *Istituto per le Tecnologie Applicate ai Beni Culturali, CNR, Roma, Italy*

([2]) *Dipartimento di Scienze Fisiche, Università di Napoli «Federico II», Napoli, Italy*

Abstract

A combined survey using ground penetrating radar, self-potential, geoelectrical and magnetic methods has been carried out to detect near-surface tombs in the archaeological test site of the Sabine Necropolis at Colle del Forno, Rome, Italy. A 2D data acquisition mode has been adopted to obtain a 3D image of the investigated volumes. The multi-methodological approach has not only demonstrated the reliability of each method in delineating the spatial behaviour of the governing parameter, but mainly helped to obtain a detailed physical image closely conforming to the target geometry through the whole set of parameters involved.

Key words *applied geophysics – archaeology – integrated approach – tomographic imaging*

1. Introduction

Non-destructive geophysical methods are routinely used in archaeology to provide a detailed physical and geometrical definition of hidden features prior to excavation work. Due to the often limited size and depth of any archaeological structure, it may be rather difficult to single out position and extension because of the generally low signal-to-noise ratio (S/N). It is possible to tackle such a difficulty by improving data acquisition and processing techniques and mainly integrating different geophysical methods.

In this work we present the results of a multi-methodological survey carried out for detecting superficial cavities (tombs) in the archaeological park of the Sabine Necropolis at Colle del Forno, Rome (see fig.1). We have integrated Ground Probing Radar (GPR), Self-Potential (SP), dipolar geoelectric and magnetic techniques and results.

2. The archaeological test site

The Sabine Necropolis at Colle del Forno, located on a SE-NW oriented oblong hill along the Tiber valley near Rome, Italy, is characterised by the presence of numerous *dromos* chamber tombs, most of them still unexplored.

Geologically, the studied area is formed by a series of lithoid tuffs about 10 m thick, with resistivity values of about 30 $\Omega \cdot$ m, overlying Pleistocene-Quaternary sandy-clayey sediments. The tuffs are covered by a layer of 20-30 cm

Mailing address: Dr. Fabio Cammarano, Istituto per le Tecnologie Applicate ai Beni Culturali, CNR, Via Salaria km 29,300, 00016 Monterotondo St., Roma, Italy; e-mail: camma@na.infn.it

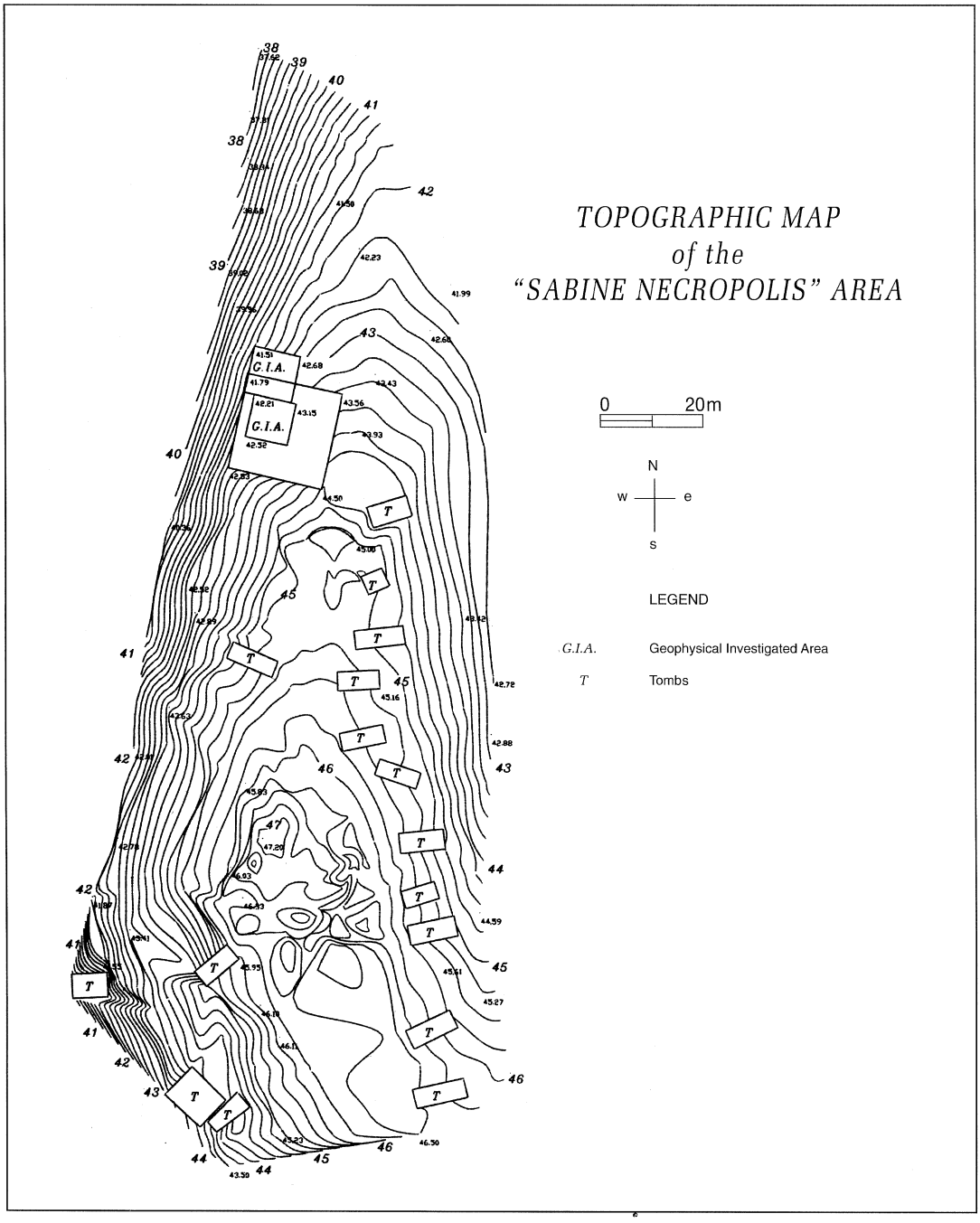

Fig. 1. Topographic map of the Sabine Necropolis at Colle del Forno (Rome) with location of the survey areas.

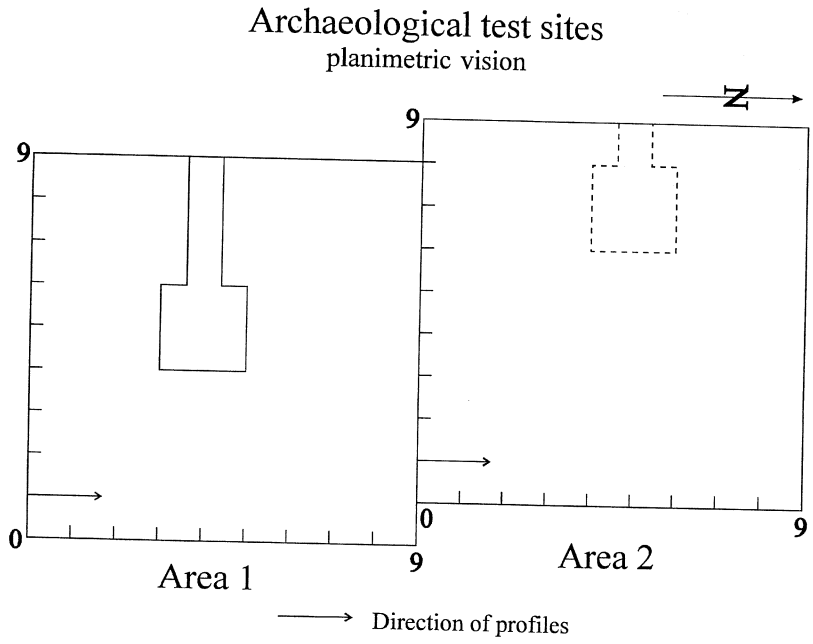

Fig. 2. Plan view of the survey Area-1 and Area-2 with location of the expected tombs.

thick top soil. From the results of archaeological studies (Santoro, 1977) the tombs can be assimilated to cavities with a standard volume of $2 \times 2 \times 1.5$ m^3, sometimes even greater. The roof is normally found at a depth of about 0.8-1.0 m below the ground surface. Each tomb presents a *dromos* (entrance corridor) of 6 m in length at most, and roughly with a 1×1 m^2 cross-section.

We have chosen two still unexplored zones, indicated as Area-1 and Area-2, where two tombs are believed to exist. Both areas have size of 9×9 m^2 and the expected tombs should be located as in fig. 2, according to the ancient excavation technique.

3. The GPR survey

In both Area-1 and Area-2 a regular grid made of 46 south-northward stretching parallel profiles, each 9 m long, was surveyed by GPR. Along each profile, the measurements were regularly carried out every 20 cm. The spacing between adjacent profiles was also 20 cm. The radar traces were collected in a 0-100 ns time window in true amplitude mode without any filtering and gain. The velocity of the electromagnetic waves in that ground is 7.5 cm/ns (Malagodi *et al.*, 1996).

The radar system consisted of a GSSI SIR-10 with 16 bits dynamic range, 1024 samples per scan and 8 stacks. The system was equipped with antennas operating at 100 MHz and the bistatic mode with a spacing of 95 cm was adopted. The GPR data were transferred and elaborated using the GSSI Radan-3 software. In order to carry out signal processing, the field data were finally converted from Radan format to SEG-2 seismic format and then processed using Seistrix 3 Interpex software.

All the collected traces showed low-frequency noise, most probably due to ground-antenna coupling, and consequently a low S/N ratio. To attenuate the disturbance due to low

and high-frequency noise and enhance the S/N ratio a band-pass filter was applied.

Finally, to obtain a planimetric vision a time-slice representation was applied using all processed profiles. A time-slice represents a cut at a specified time across the radar scan, reported as a function of the x and y horizontal coordinates. The final drawing is a contour of the radar intensities at the specified time value across parallel profiles. Also, to have the depth progression of the anomalies, *i.e.* the 3D body geometry pseudo-image, a regular sequence of time slices was edited for increasing times with such a constant time interval as to realise the most complete image definition.

Figure 3a,b shows the results of the time-slice representation corresponding to different two-way-travel time (*twt*), respectively for Area-1 and Area-2.

4. The SP survey

The SP method has seen in the past a rather limited use in archaeology (Wynn and Sherwood, 1984). The reason was usually ascribed to the low SP anomalies close to archaeological structures and to the difficulty of data acquisition, due to the apparent instability of the natural electric signal, either in the form of rapid fluctuations or as slow trends. Generally, the anomalies do not exceed a few tens of mV (Corwin, 1990). Now, the availability of a computer-aided light field technology makes feasible the collection of a very dense data grid and the use of sophisticated averaging and processing techniques.

Many physical models have been suggested to explain natural electric currents. In particular, SP anomalies generated by shallow sources,

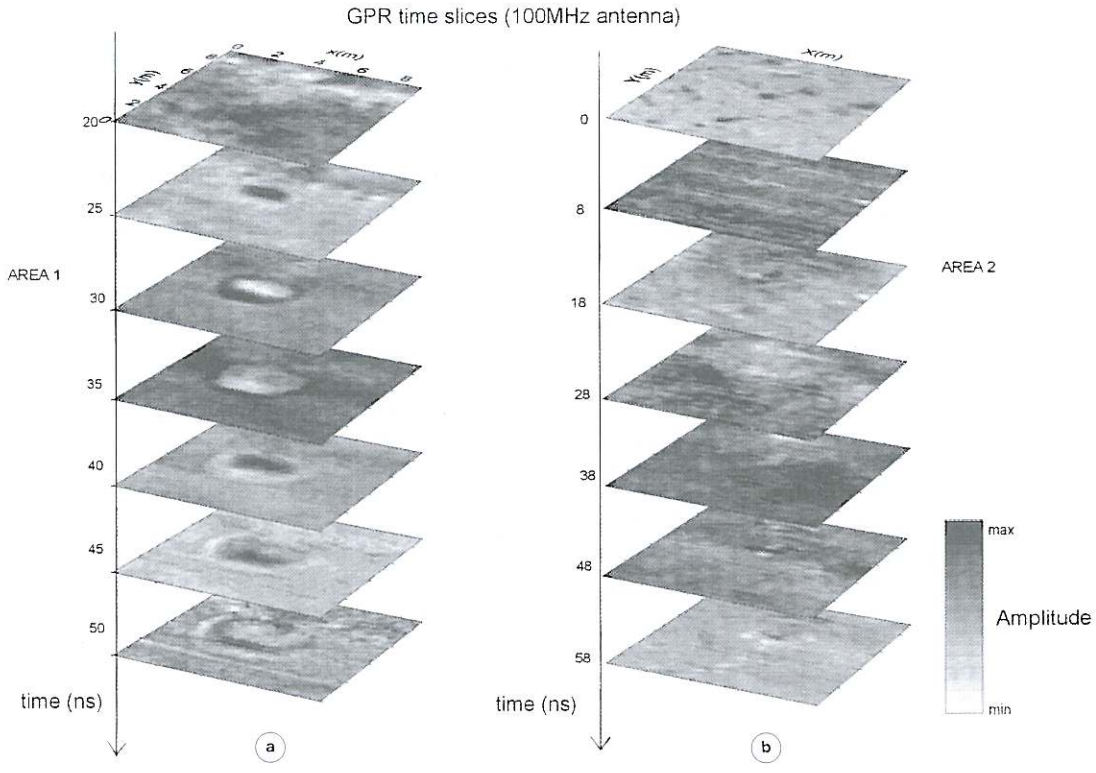

Fig. 3a,b. Ground penetrating radar time slices (100 MHz) for Area-1 (a) and Area-2 (b).

as those related to archaeological structures, can be included within the streaming potential phenomenology, provided that mineralisation potentials can be excluded, as is often the case.

The SP acquisition in the test site was made using the potential technique, which consists in keeping fixed an electrode, say the reference electrode, and moving the other, say the mobile electrode, along a straight profile. To minimise electrode polarisation spurious effects we employed standard copper-copper sulphate porous pots.

We used a sampling interval of 0.5 m along the profile, which was taken parallel to the x-axis. The measurements were collected along parallel profiles with offset distance of 0.5 m along the y-axis. Finally, by calculating the potential drops ΔV between adjacent points along the x-direction and dividing them by the constant electrode spacing $\Delta x = 0.5$ m, we obtained a 2D matrix of the x-component of the natural electric field.

The knowledge of the true distribution of polarised electrical charges underground, producing the observed SP field, requires sophisticated analysis procedures. Indeed, due to the capillary diffusing nature of the streaming phenomenology and to the general inhomogeneous structure of the buried volumes, the SP sources can be of two different types. The first type refers to the SP primary sources, *i.e.* the charge polarisation caused by the combined action of the ion adsorption capacity of the rock matrix and the electrokinetic flow through rock pores and fissures. The second type relates to the SP secondary sources, *i.e.* the continuous distribution of induced charges which accumulate across resistivity discontinuities. Both primary and secondary SP sources can be located anywhere underground in an unpredictable way.

To obtain information about the SP source distribution, we adopted the tomographic imaging method proposed by Patella (1997). Briefly, the method is as follows.

The estimated component of the natural electric field, say $E_x(x, y)$, is cross-correlated with the function $\Im_x[x-x_q, y-y_q, z_q]$, representing the SP synthetic response of a scanning elementary positive charge with unitary intensity located in the subsurface at any generic point with coordinates (x_q, y_q, z_q), *viz.*

$$\Im_x[x-x_q, y-y_q, z_q] = \\ = \frac{(x-x_q)}{\{(x-x_q)^2+(y-y_q)^2+z_q^2\}^{3/2}}. \tag{4.1}$$

Then, by a normalisation procedure of the cross-correlation operator based on Schwarz's inequality a charge occurrence probability function $\eta(x_q, y_q, z_q)$ is defined as

$$\eta(x_q, y_q, z_q) = \\ = Cz_q \int_{-\infty}^{+\infty}\int_{-\infty}^{+\infty} E_x(x, y)\,\Im_x(x-x_q, y-y_q, z_q)\,dx\,dy, \tag{4.2}$$

where

$$C = 2\left[\pi \int_{-\infty}^{+\infty}\int_{-\infty}^{+\infty} E_x^2(x, y)\,dx\,dy\right]^{-1/2}. \tag{4.3}$$

The function $\eta(x_q, y_q, z_q)$ is interpreted as the probability that a charge located at a point x_q, y_q, z_q be responsible of the SP field observed on the ground surface. As it is $-1 \le \eta(x_q, y_q, z_q) \le +1$, the procedure can be used to search in an objective way the most probable localisation of the polarised negative and positive charged nuclei in the subsoil.

The above numerical SP data processing allowed us to obtain a 3D matrix of charge occurrence probability values. We were thus able to draw a set of horizontal slices relative to different levels, each showing the distribution of the probabilities at a given depth. Figure 4a,b shows the results of the SP tomographies for the two investigated areas.

5. The dipolar geoelectric survey

In archaeology the occurrence of an anomalous resistivity high is a good indicator of the presence of a cavity (tomb) hosted within a

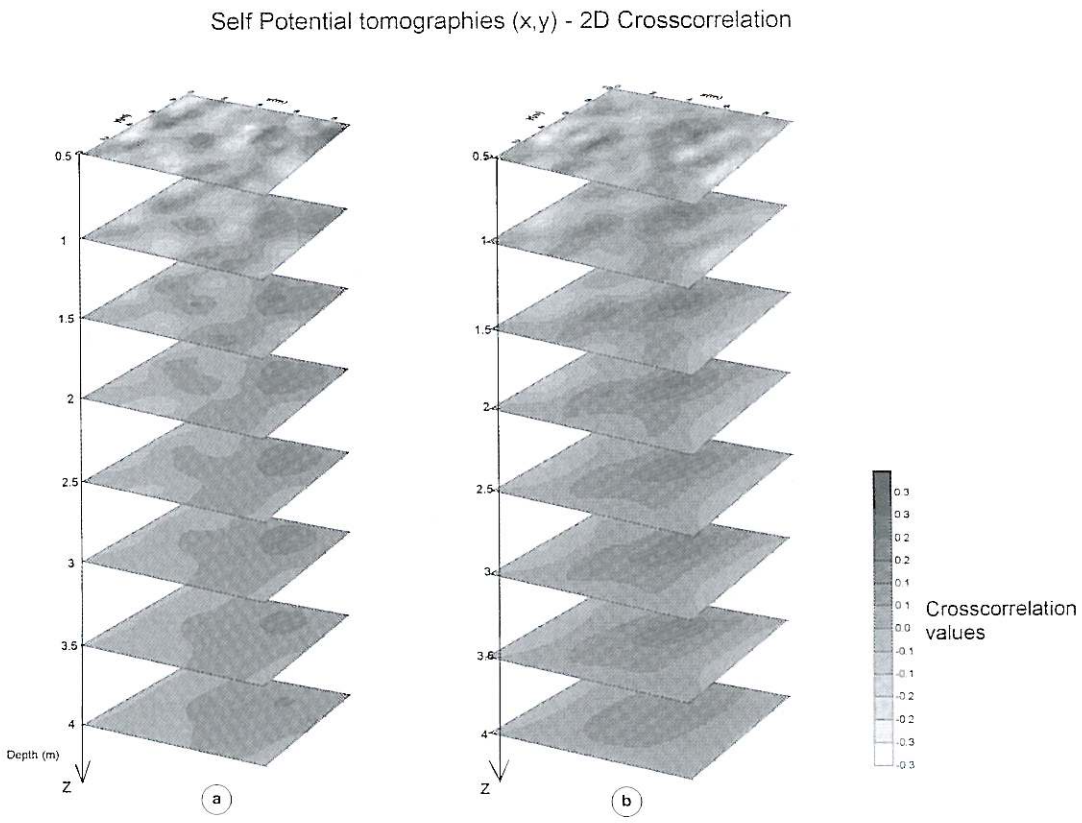

Fig. 4a,b. Self-potential tomography for Area-1 (a) and Area-2 (b).

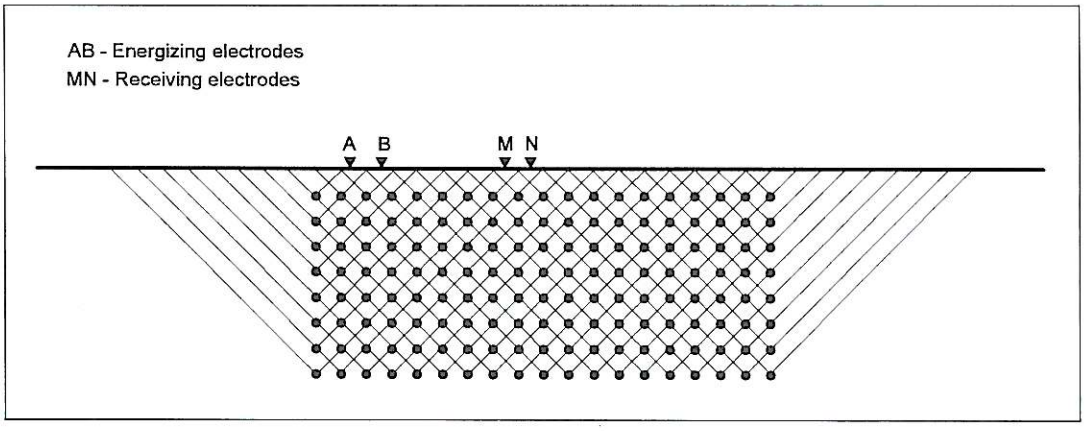

Fig. 5. Sketch of the geoelectric dipole-dipole pseudosection method. AB and MN are the emitting and receiving dipoles, respectively.

less resistive material. Of course, the presence of ionised waters within the hosting rock notably favours target detectability as it enhances the resistivity contrast. On the other hand, the occurrence of an anomalous resistivity low can be indicative of the presence of some very conductive structure, as a ditch in sound rock filled with fine sediments, or a water or clay filled cavity.

To achieve a high resolution survey, we used the dipole geoelectric pseudosection technique along selected profiles. This technique is considered a first-order tomography (Worthington, 1984), as it can lead to symptomatic resistivity anomaly images across the investigated section. Figure 5 shows a sketch of the adopted configuration for each profile.

In each 9×9 m^2 test area at Colle del Forno ten parallel dipole-dipole profiles were performed with a constant separation of 1 m from each other. The measurements were carried out with the BRGM SYSCAL/R2 resistivity-meter, which can work in a stacking signal enhancement mode. Each apparent resistivity datum was obtained with dipoles 0.5 m long and attributed at a pseudodepth equal to half the spacing between the centres of the emitting and receiving dipoles along the median vertical axis through the line joining them. The step-by-step continuous displacement of the dipoles along each profile provided a dense network of about 152 data points in the vertical pseudosection. The measured apparent resistivities in the ten sections of each area were then pulled together to obtain a 3D matrix. We were thus able to represent horizontal apparent resistivity slices at different pseudodepths, which are displayed in fig. 6a,b, respectively for Area-1 and Area-2.

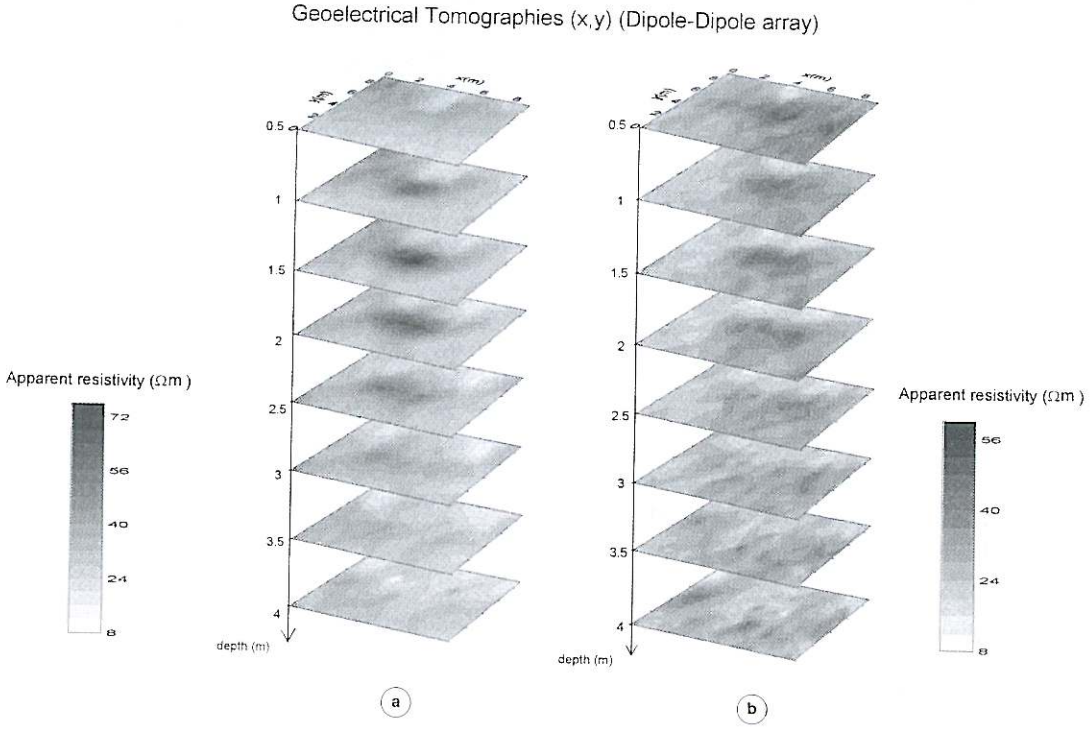

Fig. 6a,b. Dipolar geoelectric tomography for Area-1 (a) and Area-2 (b).

6. The gradiometric survey

In archaeology the magnetic method is frequently employed, for it can provide very useful information on the presence and localisation of ancient remains of anthropic origin having high susceptibility contrast against the hosting material (Wynn, 1986). Significant contrasts can also be generated by lacking masses as are cavities (tombs). The gradient array facilitates the detection of shallow and small features.

In the Sabine Necropolis the GEOSCAN FM 36 fluxgate gradiometer was used. This instrument measures the gradient of the vertical magnetic component Z with a fixed inter-sensors vertical spacing of 0.5 m. In order to perform a unique survey and hence draw a unique gradiometric map, both Area-1 and Area-2 were enlarged by 1 m along the western and eastern side, respectively. Area-2 was also extended by 2 m to the north. The final dimension of the assembled area was 10×20 m^2, wherein we recorded 21 parallel S-N profiles spaced 0.5 m apart, each 20 m long. The measurements were again collected with a sampling interval of 0.5 m along each profile. The bottom sensor of the gradiometer was taken at the constant height of 30 cm above the ground.

After despiking, filtering and reranging, the data were finally assembled in a unique contour map of the residual values of the gradient of Z, including both areas (see fig. 7).

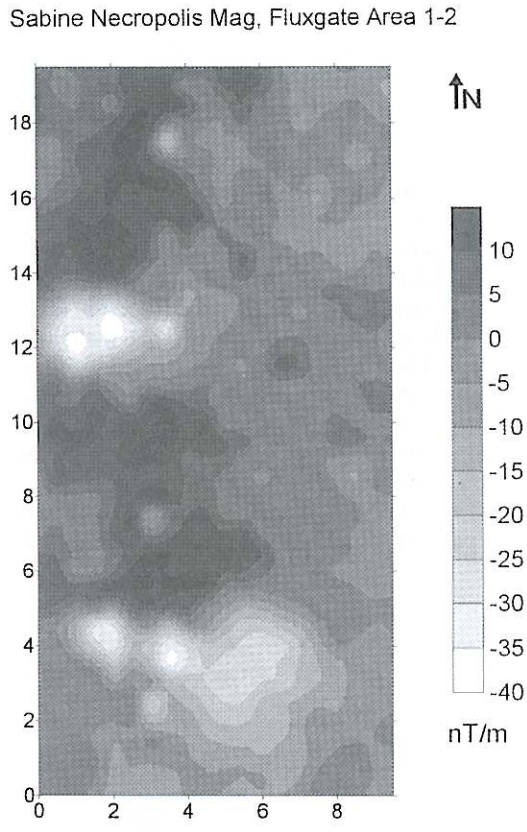

Fig. 7. Residual contour map of the gradient of the vertical magnetic component.

7. Discussion

7.1. *Analysis of the GPR time-slices*

The GPR results obtained in Area-1 (fig. 3a) show a clear anomaly ascribable to the presence of a tomb. The *twt* of 25 ns would correspond to the top, approximately 90 cm deep. The *twt* of 30, 35 and 40 ns, approximately corresponding to the depths of 1.5, 2 and 2.5 m, respectively, are likely to match the inner part of the cavity. Finally, the *twt* of 45 ns would correspond to the bottom of the tomb, approximately 3 m deep. No evidence of the corridor emerged.

On the contrary, the time-slices in Area-2 (fig. 3b), which are probably affected by a very high level of scattering disturbances, do not show any evident anomaly. This can be due either to lack of a tomb, or to its existence but in bad state of conservation, due to the collapse of the roof and accumulation of lithoid blocks and sediments inside.

7.2. *Analysis of the SP tomographies*

In Area-1 (fig. 4a) we observe various SP source centres, all very shallow at about 1 m of depth. Two positive probability highs extended in the y-direction appear in correspondence of

$x = 2$ m and $x = 6$ m. Another positive probability high appears amid the two previous ones, but at a lower position along the y-axis, around $y = 4$ m. The set of these three nuclei could be ascribed to the lateral walls of a cavity, where secondary SP sources of electrokinetic origin may accumulate. Another SP anomaly, located in the right high corner, may be probably due to a near-surface exotic border effect.

In Area-2 (fig. 4b) a sequence of positive spots of the η-function, propagating down to a depth of 2.5 m below ground level, appears within the central portion of the survey area with a rough shape of a tuning fork. The toothed profile of the anomaly would contour the lateral boundary of a chamber tomb, at least partially filled, while the upper handle of the anomaly would correspond to the northern lateral boundary of the *dromos*.

7.3. *Analysis of the geoelectrical tomographies*

In Area-1 (fig. 6a) we easily recognise a neat resistivity high around 75 $\Omega \cdot$ m in the depth range between 1 m and 2 m. Such a feature can of course be related to an empty cavity. Moreover, a shallower resistivity low, very well evident in the first section at the pseudo-depth of 0.5 m, can be interpreted as the effect of the presence of the *dromos*, filled, however, with conductive fine sediments.

Similar features are revealed in Area-2 (fig. 6b), but apparently with smaller resistivity contrasts. In particular, the resistivity high, likely representing a cavity, does not exceed this time 56 $\Omega \cdot$ m and does not show a well contoured geometry. This evidence would again suggest a not perfect state of conservation of the expected cavity.

7.4. *Analysis of the gradiometric surface map*

The gradiometric contour map in fig. 7 clearly shows the existence of two minima of similar kind. The first anomaly, located in Area-1, shows a more extended halo than the second one, located in Area-2. In both cases, the very intense negative nucleus can be likely ascribed to a buried structure showing negative susceptibility contrast with respect to the surrounding material. This is particularly true in the case of an empty cavity.

In Area-1, as the minimum closely corresponds to the anomalies obtained with the other methods, there should be no doubt about the presence of a well preserved tomb. The imprint of the corridor-plus-chamber system appears very nicely contoured.

In Area-2, however, the minimum extends over a more restricted area and would better delineate the entrance corridor to a cavity, most probably filled with very low susceptibility material, as is often the case.

7.5. *Integrated geophysical analysis*

By comparing all the results shown by each single method, the following integrated interpretations can be made for the two areas.

In Area-1 all methods concur to give the global image of an intact chamber tomb with the *dromos* filled however with fine sediments. In fact, GPR, dipole geoelectric and gradiometric data show quite matching anomalies corresponding to the inner chamber. This picture is also well framed by the SP anomaly which appears located all around the chamber, thus defining its boundary. The standard dimensions of the cavity are then confirmed by the 3D tomographic representation. Concerning the entrance corridor, the same methods show such contrasting effects as to be justified by an elongated body filled with conductive fine sediments of no magnetic relevance and vanishing *em* wave reflectivity. Indeed, a reversed resistivity contrast, compared with that of the nearby empty chamber, would be more than sufficient to explain both the resistivity low narrow zone and the charge self-accumulation at its boundary.

In Area-2 the situation appears somewhat more problematic. Absence of GPR signals and of a gradiometric minimum in the zone where a resistivity small high occurs surrounded by SP charge accumulations, would be indicative of a chamber body very likely filled with collapsed tuff blocks from the top. Such a

filling would be enough to obliterate any GPR and magnetic contrast, though leaving sufficient residual voids as to induce some geoelectric and SP response. For the *dromos*, the same considerations as above apply equally well.

8. Concluding remarks

Taking into account the results obtained by the integrated survey, it is possible to make the following two final considerations:

1) The 2D high-resolution data acquisition technique conditions the investigated area with a very high number of measurements. This procedure allows a set of detailed information to be collected on the lateral extensions of the anomalous bodies, which are normally not available by the traditional sampling intervals.

2) The improvement of the processing techniques towards a 3D tomographic imaging and the integration of different geophysical methods enable one to better define position, extension, depth and thickness of any anomalous body (archaeological remnant) within the geological context. Also, the discrimination power between close but distinct archaeological structures is notably enhanced.

REFERENCES

CORWIN, R.F. (1990): The self-potential method for environmental and engineering applications, in *Geotechnical and Environmental Geophysics*, edited by S.W. WARD, vol. 1: *Review and Tutorial*, SEG, Tulsa, 127-146.

MALAGODI, S., L. ORLANDO, S. PIRO and F. ROSSO (1996): Location of archaeological structures using GPR method. 3D data acquisition and radar signal processing, *Archaeol. Prospect.*, **3**, 13-23.

PATELLA, D. (1997): Introduction to ground surface self-potential tomography, *Geophys. Prospect.*, **45**, 653-681.

SANTORO, P. (1977): Colle del Forno, loc. Montelibretti (Roma). Relazione di scavo sulle campagne 1971-1974 nella necropoli, in *Atti Accad. Naz. Lincei*, **31**, 211-298.

WORTHINGTON, M.H. (1984): An introduction to geophysical tomography; *First Break*, **2**, 20-26.

WYNN, J.C. (1986): Archaeological prospection: an introduction to the special issue, *Geophysics*, **51**, 533-537.

WYNN, J.C. and S.I. SHERWOOD (1984): The Self-Potential (SP) method: an inexpensive reconnaissance and archaeological mapping tool, *J. Field Archaeol.*, **11**, 195-204.